Regular Article

PHYSICAL CHEMISTRY RESEARCH
Published by the
Iranian Chemical Society
www.physchemres.org
info@physchemres.org

Phys. Chem. Res., Vol. 12, No. 3, 709-727, September 2024
DOI: 10.22036/pcr.2024.416266.2415

A Spectroscopic and Molecular Docking Study on the Interaction of 2′-Hydroxyflavanone with Bovine Serum Albumin

M. Patar, A. Jalan and N. Shaemningwar Moyon*

Department of Chemistry, National Institute of Technology Silchar, Cachar, Assam-788010, India

(Received 13 September 2023, Accepted 27 January 2024)

Flavonoids have a broad area of anatomical interest and as such, it is vital to understand their association behavior with proteins. Here, under biological conditions, the interaction of 2′-hydroxyflavanone (2HF) with cattle protein (BSA) was investigated using steady-state UV-visible and fluorescence spectroscopy, FT-Infra Red spectroscopy, circular dichroism, and docking investigations. Analysis showed static quenching of BSA in the presence of 2HF. FRET analysis showed possibilities of energy transfer between 2HF and BSA. Experiments and molecular docking results indicate that 2HF binds to subdomain IIA of BSA. The thermodynamic parameters like $\Delta H0$, $\Delta S0$, and $\Delta G0$ indicate that the association with 2HF is spontaneous, exothermic, and involves van der Waals force and H-bonding. By using FTIR and CD investigations demonstrate structural changes in BSA following a drug interaction. The conformational and functionality change of serum albumin (BSA) after association with the drug is further depicted by esterase-like activity study of serum albumin in the presence of 2HF. The binding of the BSA-2HF complex decreased in the presence of selected metallic ions.

Keywords: Flavonoids, Protein, Fluorescence quenching, Föster resonance energy transfer, Static quenching

INTRODUCTION

Flavonoids are a broad class of phenolic plant components that have been known to possess bioactive potential like antioxidants, anti-inflammatory, anticancer, and antiproliferative properties [1-4]. The constituent of flavonoids is two six-membered aromatic rings and one oxygen-containing pyrene ring. The Structural activity studies revealed that the number of hydroxyl groups present in flavonoids determines their activity. Flavonoids containing more than one hydroxyl group exhibit greater antioxidant and anti-inflammatory activities whereas, those which have zero or one hydroxyl group as a substituent have greater anticancer properties than flavonoids with multiple hydroxyl groups [5].

2′-Hydroxyflavanone (2HF) as shown in the scheme, belongs to a family of flavonoids with one hydroxyl group and is mostly found in oranges and citrus fruits. Several studies on the anticancer properties of 2HF *in vitro* have been reported. For example, 2HF prevents cancer cell growth in the human, renal, colon, and breast, [6,7] and prevents the spread of human lung carcinoma A549 cells [8,9] and VHL-mutant RCC [6,10]. Recently, 2HF was found to hinder the prime key of breast cancer including RLIP76, ER-alpha, and HER2 [11]. It was also reported that 2HF enhances the anticancer properties of other anticancer drugs [9]. 2HF has shown various biological activities making it vital to investigate its interaction with serum albumins. Moreover, Jianbo Xiao *et al.* [12] reported that the binding energy of flavanones with proteins increased to a great extent in the presence of single hydroxyl group in the A ring. However, the presence of more hydroxyl groups in the same ring shows decrease in the binding energy. However, no work has been reported on the interaction of flavanones containing hydroxyl groups at the B ring with albumins. The study of 2HF will further reveal insights into the interaction of BSA with

*Corresponding author. E-mail: nsmoyon@che.nits.ac.in

flavanones containing a hydroxyl group in the B ring.

Highly prevalent plasma proteins known as serum albumins transport a variety of exogenic and endogenic chemicals through the blood [13,14]. They have the potential effect to bind with a variety of acceptors like drugs, metal ions, steroids, amino acids, and fatty acids [15]. Bovine serum albumin (BSA) is a more common and largely studied serum albumin because it is easily available, low cost, and homologous to HSA [16]. The nature of the binding of ligands to BSA affects their therapeutic efficiency [17-20]. Therefore, it is significant to investigate the nature and thermodynamics of the interaction between donor and acceptor to understand the effect and action of the acceptor molecule. Moreover, understanding the interaction on a molecular basis will be of great importance in designing new drugs with improved efficiency of their specific action [21].

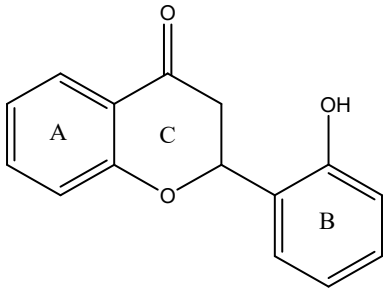

Scheme. Chemical structure of 2′-hydroxyflavanone

The current study deals with the binding analysis of 2HF with Serum Albumin using steady-state UV-visible and emission spectroscopy, FT-infrared spectroscopy, CD spectroscopy, and molecular docking. The quenching constants, energies of binding, binding sites, the distance between the 2HF and serum albumin, and the force responsible for binding were determined. To confirm the binding sites, docking data and site-selective binders ibuprofen (for site II) and warfarin (for site I) were utilized. The effect of bivalent metal ions on the binding properties was also examined. The information gathered in this study will not only reveal the nature of the interaction of 2HF with BSA but will also be of great importance in the field of drug design.

MATERIALS AND METHODS

Chemicals

The serum albumin (BSA) (MB083-5G) was procured from HiMedia Laboratories. 2′-Hydroxyflavanone (CAS no.: 17348-76-4), warfarin (CAS no.: 81-81-2), and ibuprofen (PHR1004, CAS no.: 15687-27-1) were obtained from Sigma-Aldrich and used as it is. $CuCl_2$ and $CaCl_2$ were purchased from Fisher Scientific whereas $FeCl_2$ was obtained from Merck to be used as a source of bivalent metal ions. NaH_2PO_4 and Na_2HPO_4 were purchased from Fisher Scientific and Millipore water was utilized all through the process.

Sample Preparation

Using a buffer of pH = 7.0, the stock solutions of BSA (1×10^{-4} M) and a sparingly soluble 2HF (1×10^{-4} M) were made. From the stock solution, all the working solutions were prepared by fixing BSA's concentration at 3×10^{-6} M, while 2HF's concentration varied from 0.0, 2.2, 4.4, 6.6, 8.8, 11, 14, 17, and 22 ($\times 10^{-6}$ M) respectively.

Methods

Cary-Bio100 absorption spectrophotometer was employed to measure the absorption spectra within 200-500 nm. The emission spectra of BSA were recorded using a spectrofluorimeter (Hitachi, F-4600) using a 10 mm quartz cuvette cell. The spectrofluorimeter constitutes a thermostatic cell holder and a 150W Xenon lamp for the source of light. It was also fitted with a water circulatory bath. Both the excitation and emission slits were set at 5 nm, with a 240 nm per min scan speed. By using the following Eq. (1), all the emission spectra of the serum albumin were adjusted to prevent the inner filter effect.

$$F_{cor} = F_{obs} \times 10^{(A_1+A_2)/2} \quad (1)$$

Where, F_{corr} *and* F_{obs} designate the protein's resolved fluorescence spectra and the fluorescence spectra at different doses of 2HF, A_1 and A_2 designates the total absorbance of 2HF corresponding to the wavelength at 280 nm and ~340 nm, respectively [22].

The CD spectra were generated at 298 K with J-1500 spectropolarimeter in 0.1 cm path length. All spectra were

collected within the 200-250 nm wavelength range with a data interval of 0.5 nm at 50 nm min^{-1}. 3×10^{-6} M BSA concentration was chosen and the concentration of 2HF was varied in the ratio of 1:3 and 1:4. The experiment was conducted using a buffer (pH = 7.0). The result is computed as ellipticity (mdeg) using the circular dichroism tool.

The Infrared spectroscopy analysis was carried out at 298 K using an FTIR spectrometer (Bruker) equipped with a diamond-attenuated complete reflection method in both the presence and absence of the drug (2HF). The amide moiety of the peptide chain namely Amide I and Amide II are responsible for interaction. The IR spectra were collected within the 500-4000 cm^{-1} wavelength range by fixing the molar amount of BSA at 3×10^{-6} M and that of 2HF at 2×10^{-5} M.

To further explore the possibility of conformational and functionality change in BSA upon binding with 2HF, the esterase-like activity of serum albumin (BSA) was conducted with p-nitrophenyl acetate (PNPA) as a substrate by using a Cary-Bio100 spectrophotometer. The optical density of the released product p-nitrophenol was measured at a wavelength of 400 nm [23] by using a 10 mm quartz cuvette. At 37 °C in a solution of buffer with a pH of 7.0, a 3 μM solution of BSA, PNPA (100, 200, 300, 400, 500, 600, and 700 μM), and 2HF (2.2, 4.4, and 22 μM) was taken in the reaction mixture. The molar absorptivity $\varepsilon = 17.700$ M^{-1} cm^{-1} was used for p-nitrophenol in all reactions for BSA. At the wavelength of 280 nm, protein concentration is determined spectroscopically by using extinction coefficient 49833 M^{-1} cm^{-1} on Cary-Bio100 as reported by Chandel *et al.* on Perkin Elmer Lambda 25 UV/VIS [24]. The initial velocities (υ_0) of the reactions were determined from the slope of the plot between 0 to 7 min [25].

The molecular docking study of the optimized structure of 2HF and serum albumin (BSA) was performed using The Scripps Research Institute's Auto Dock 4.2 [26]. The geometry of 2HF was assembled utilizing Chem.3D ultra (version 8.0, CambridgeSoft.Com, USA) and was optimized using Gaussian 09 [27] software package at the theoretical level of 6-31G(d,p/B3LYP) [28]. Furthermore, from the only positive values obtained in frequency calculations using the same theory, we can infer that the optimized stationary point is a local minimum. The structure of BSA (PDB: 3V03, http://doi.org/10.2210/pdb3V03/pdb) having a 2.70 Å resolution was downloaded from the Protein Data Bank (https://www.rcsb.org/). Firstly, BSA was freed from water molecules. Then polar hydrogens were added and partial atomic charge77 was calculated for 2HF and BSA using Gasteiger-Marsili [29] and Kollman methods [30]. On performing blind docking, 2HF goes to chain A, hence docking was done again using chain A of BSA and grid maps of dimension (120 × 90 × 110) with a grid-point spacing of 0.7 Å, centered at coordinates x = 37.941, y = 21.097, and z = 36.088 were defined for calculations in Auto-grid [31]. For determining the binding energies between BSA and 2HF, docking was run using the Lamarckian genetic algorithm. All the parameters were set to default and the clusters were sorted based on root-mean-square deviation (rmsd) tolerance of 2.0 Å between all probable conformations, amongst which the one with minimum binding energy was adopted for further investigation.

RESULTS AND DISCUSSION

2HF Quenches the Fluorescent Properties of BSA

The serum albumin emission spectra were measured by fixing the excitation wavelength at 280 nm at five different temperatures 298, 303, 308, 313, and 318 K respectively. The effect of higher temperature has been described as well from the changes in protein helical structure changes as reported in Kunio *et al.* 1989 [32].

The fluorescence intensity of BSA gradually decreases with a subsequent increase in the concentration of the 2HF at all temperatures (Fig. 1). This quenching of fluorescence intensity of BSA by 2HF suggests that there is an interaction between the drug and protein molecule. It is also observed from Fig. 1 that there is no change in the emission maxima of Bovine serum albumin in the presence of 2HF. This indicates that the microenvironment surrounding trp-214 is not affected by the presence of 2HF [33].

Stern-Volmer Analysis

Several molecular interactions such as molecular rearrangement, excited state reaction, ground-state complex formation, collisional quenching, and energy transfer are responsible for the fluorescence quenching process [33]. However, commonly discussed mechanisms are static and collisional or dynamic quenching [34].

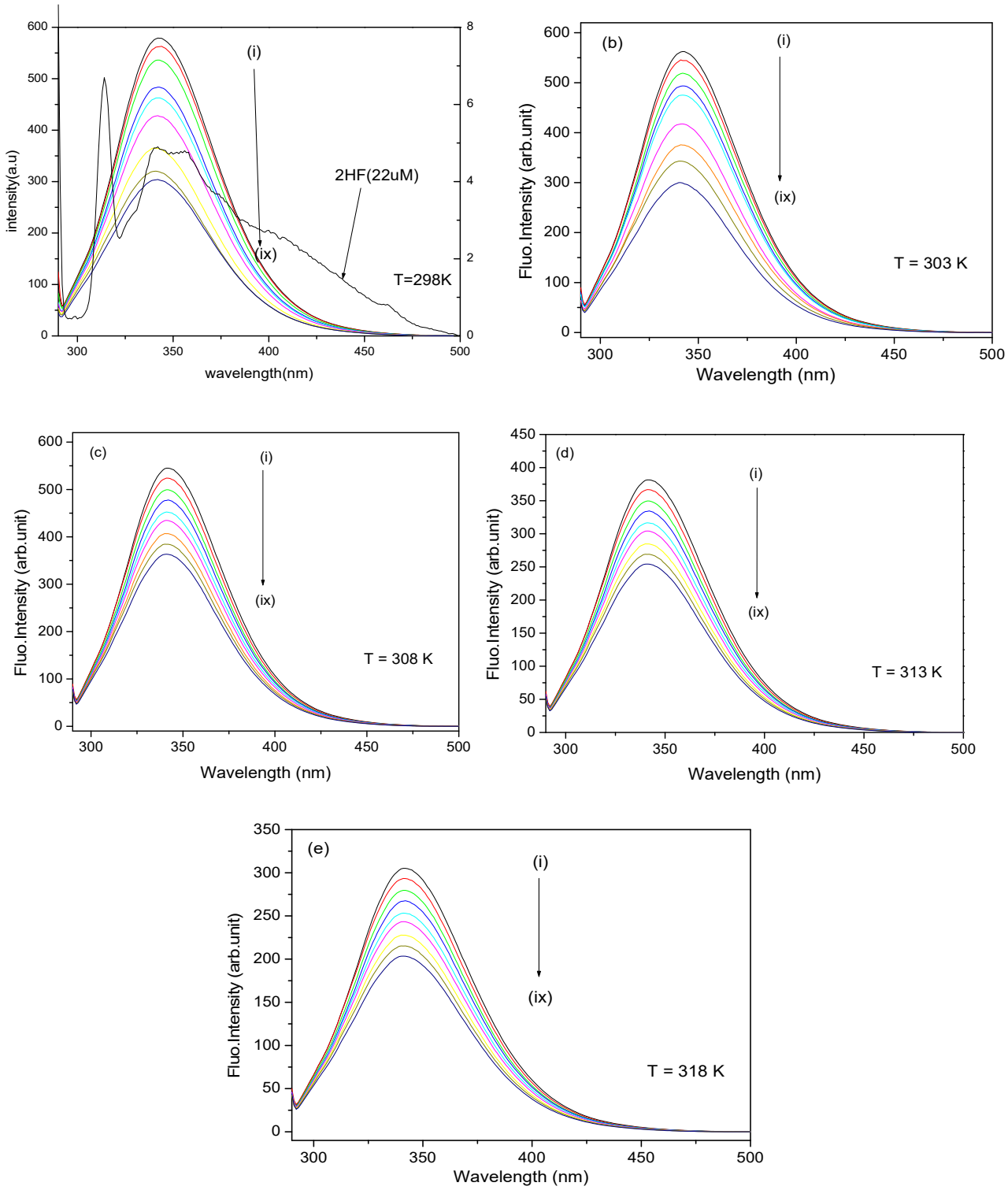

Fig. 1. Emission spectra of serum albumin in the presence of 2HF at (a) 298 K (emission spectra of 2HF only) (b) 303 K (c) 308 K (d) 313 K and (e) 318 K. [BSA] = 3 ×10^{-6} M; [2HF] = (i) 0 (ii) 2.2 (iii) 4.4 (iv) 6.6 (v) 8.8 (vi) 11(vii) 14 (viii) 17 (ix) 22 (× 10^{-6} M), λ_{exc} = 280 nm.

Static quenching is responsible for non-fluorescent ground-state compound formation between the 2HF and the BSA. On the other hand, dynamic quenching results from the collision of the quencher and the excited state probe [35]. The mechanism of quenching is best examined with Stern-Volmer Eq. (2) given below [36].

$$\frac{F_0}{F} = 1 + k_q\tau_0[Q] = 1 + K_{SV}[Q] \qquad (2)$$

Where, the fluorescence intensities F_0 and F denote the free and bound state of the quencher, respectively. τ_0, $[Q]$, k_q, and K_{SV} are the decay time of the unquenched probe, quencher concentration, the quenching rate constant, and the Stern-Volmer quenching constant respectively. The plot of F_0/F versus [Q] at different temperatures is given in Fig. 2 and the corresponding values are presented in Table 1. As visible, the linear SV plot (correlation coefficient, R = ~0.98) signifies the presence of either static or dynamic quenching.

These two types of quenching namely static and collisional quenching can be identified by studying their interaction at different temperatures [37]. Higher temperature increases the rate of diffusion leading to more dynamic quenching [35]. In these circumstances, a rise in temperature is accompanied by an increase in the SV quenching constant (K_{SV}). While the dissociation of the ground state complex would increase with the rise in temperature and result in a decrease in K_{SV} [34]. Table 1 shows that the value of K_{SV} decreases with increasing temperature, suggesting that the fluorescence quenching of serum albumin in the presence of 2HF is associated with the development of the ground state 2HF-BSA complex. Hence, it infers that 2HF-BSA complex formation takes place via static quenching mechanism. The SV quenching constant is the association constant which directly quantifies the strength of the protein's ability to bind with 2HF. The bimolecular collisional quenching constant (k_q) was calculated using the equation $k_q = K_{SV}/\tau_o$ and is displayed in Table 1 using the biopolymer's decay time of 10^{-8} s [38]. Greater k_q values than the highest collisional quenching constant for different quenchers with the biopolymer (2.0×10^{10} M^{-1} s^{-1}) are observed for static quenching [39]. Similar results were obtained for our system further designating the presence of the mechanism of static quenching in 2HF-BSA complexation.

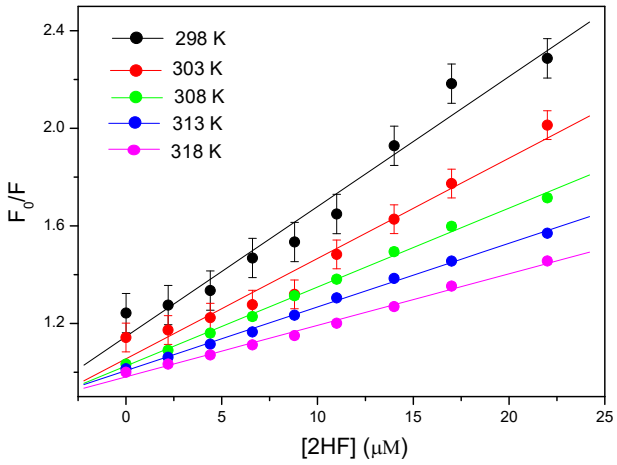

Fig. 2. Stern-Volmer plot of BSA quenching with 2HF at three temperatures.

Table 1. Results of Stern-Volmer Plot at Three Temperatures

T (K)	K_{SV} ($\times 10^4$ M^{-1})	k_q ($\times 10^{12}$ $M^{-1}s^{-1}$)	R
298	4.662 ± 0.347	4.662	0.983
303	4.243 ± 0.299	4.243	0.987
308	2.428 ± 0.055	2.428	0.997
313	2.283 ± 0.044	2.283	0.998
318	2.113 ± 0.065	2.113	0.996

Number of Places for Binding and Binding Constant

Equation (3), which was used to calculate the binding parameter (K_a) and the total number of binding locations (n) for several ligand-protein interactions, has been effectively applied to explain the equilibrium between the unbound and bonded state of quencher molecules. The K_a is a measure of the strength of protein-ligand interaction [40-45].

$$log\,\frac{F_0-F}{F} = nlogK_a + nlog\left([Q] - \frac{F_0-F}{F_0}[P]\right) \qquad (3)$$

Where the emission intensities F_0 and F denote the corresponding free and bound state of the quencher. $[Q]$ is the molar amount of 2HF and that of serum albumin is denoted by $[P]$. From the graph of $log\ \{(F_0\text{-}F)/F\}$ *versus* $log\ \{[Q]\text{-}[P](F_0\text{-}F)/F_0\}$ given in (Fig. 3), the corresponding

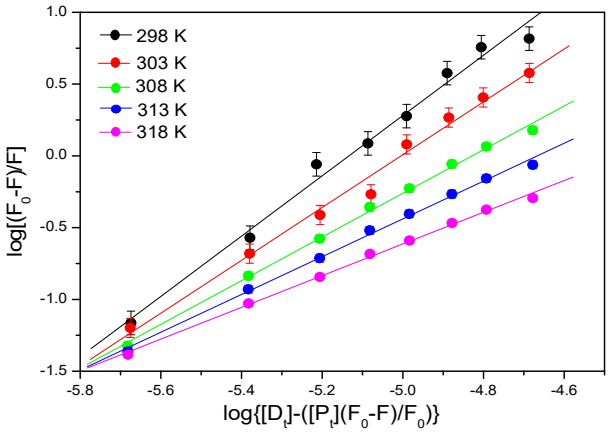

Fig. 3. Representation illustrating the ratio of log[(F_0-F)/F] to log[D]-[P](F_0-F)/F at various temperatures.

calculated values are listed in Table 2. *In vivo* studies, the flavonoids unveil moderate attachment with the drug-protein interactions having binding constants ranging from 1-15 × 10^4 (10^3 low binding constant to 10^5 high binding constant M^{-1} [46,47]. The binding constant of 2HF with BSA in the range of 10^4 M^{-1} indicates moderately strong binding which is excellent in view of showing efficacy with facile excretion (shorter elimination lifetime). Thus, it infers that under in-vivo conditions, 2HF binds moderately strongly with BSA [48,49]. Table 2 shows that the binding constant of 2HF-BSA (in the order of 10^4 M^{-1}), and the decrease in K_a at higher temperature is like K_{SV} which further shows the complexation of BSA-2HF in the ground state, again verifying the presence of static quenching phenomena. The number of binding sites is not affected by temperature and its value depicts that only one binding site of BSA is available for binding with 2HF. The binding constant as depicted as K_a calculated from the double logarithmic curve also called the association constant [45].

Thermodynamic of BSA-2HF Interaction

The drug's interaction with serum albumin is due to various factors. This includes van der Waals forces, electrostatic attraction, hydrophobic contact, and H-bonding interaction [50]. The sign and magnitude of enthalpy change (ΔH^0) and entropy change (ΔS^0) can be used to identify the force. Hydrophobic interactions are always accompanied by positive ΔH^0 and ΔS^0 while negative ΔH^0 and ΔS^0 indicate van der Waals force or H-bonding contacts. For electrostatic attraction, ΔH^0 is negative and ΔS^0 is positive [51]. To understand the binding of 2HF with BSA, the thermodynamic parameters were estimated by utilizing Eqs. (4) and (5) [52].

$$K_a = -\frac{\Delta H^0}{2.303RT} + \frac{\Delta S^0}{2.303R} \quad (4)$$

$$\Delta G^0 = \Delta H^0 - T\Delta S^0 \quad (5)$$

Where the universal gas constant R, is the temperature T, and K_a is the associative binding constant of the complex (protein-drug) at that temperature. The values of ΔH^0 and ΔS^0 were obtained from van't Hoff's plot (Fig. 4) and were used to calculate the Gibbs free energy change (ΔG^0) at all temperatures using the equation (5). The values are indexed in Table 2. The negative value of ΔG^0 and ΔH^0 implies that the interaction is spontaneous and exothermic respectively [53,54]. Both ΔH^0 and ΔS^0 are negative which indicates that 2HF is bound to BSA by van der Waals force and H- bonding attraction [55,56,57]. The large value of ΔH^0 indicates that 2HF–BSA interaction is mainly driven by enthalpy [58].

FRET Analysis on the Interaction of BSA with 2HF

The Förster resonance energy transfer or FRET can be defined as the transfer of energy between serum albumin and 2HF. It is a spectroscopic ruler and is largely utilized to measure the distance between serum albumins and the drug [59,60,61].

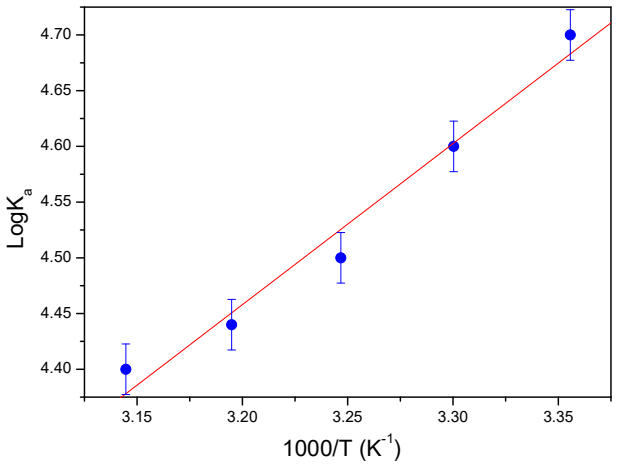

Fig. 4. The van't Hoff plot for BSA with 2HF.

Table 2: Binding Constant and Thermodynamical Parameters at Three Temperatures

T (K)	K_a ($\times 10^4$ M^{-1})	n	R^a	ΔH^0 (kJ mol^{-1})	ΔS^0 (J mol^{-1} K^{-1})	ΔG^0 (kJ mol^{-1})	R^b
298	5.25 ± 0.50	1.42	0.98	-27.668 ± 2.606	-3.180	-26.72 ± 4.16	0.98
303	4.52 ± 0.19	1.41	0.99		±0.0227	-26.70 ± 4.27	
308	2.79 ± 0.39	1.09	0.99			-26.69 ± 4.38	
313	2.82 ± 0.21	1.11	0.99			-26.67 ± 4.50	
318	2.78 ± 0.23	1.10	0.99			-26.65 ± 4.62	

R^a is the correlation coefficient for the plot using Eq. (3); R^b is the correlation coefficient for the plot using Eq. (4).

The degree of overlap in spectrum with the BSA and 2HF's emission and UV-visible spectra, as well as the protein's and drug's distance from one another, as well as the orientation of their corresponding transition dipoles, all affect how effectively energy is transferred within the serum albumin and the 2HF [20,62]. Figure 5 shows the overlay of the 2HF spectrum of absorbing radiation and the BSA luminescence spectrum.

The Förster theory's description of the transfer of energy efficiency (E) is given by Eq. (6), where r is the separation of BSA and 2HF, R_0 denotes the Förster critical distance at 50% energy transfer efficiency which is calculated using Eq. (7).

$$E = 1 - \frac{F}{F_0} = \frac{R_0^6}{R_0^6 + r_0^6} \quad (6)$$

$$R_0^6 = 8.79 \times 10^{-25} K^2 N^4 \Phi J \quad (7)$$

$$J = \frac{\int_0^\infty F(\lambda)\varepsilon(\lambda)\lambda^4 d\lambda}{\int_0^\infty F(\lambda) d\lambda} \quad (8)$$

N stands for the medium's average refractive index within the overlapping wavelength range, K^2 denotes the fluid's random orientation, which is $K^2 = 2/3$, and the quantum yield of serum albumin is denoted by ϕ. Equation (8) is used to calculate J, which is the overlap of the spectral integral of the donor's (BSA) emission spectrum and the acceptor's (2HF) UV-visible spectrum. The protein's emission intensity is $F(\lambda)$ and the molar absorptivity is $\varepsilon(\lambda)$ at wavelength λ of the drug.

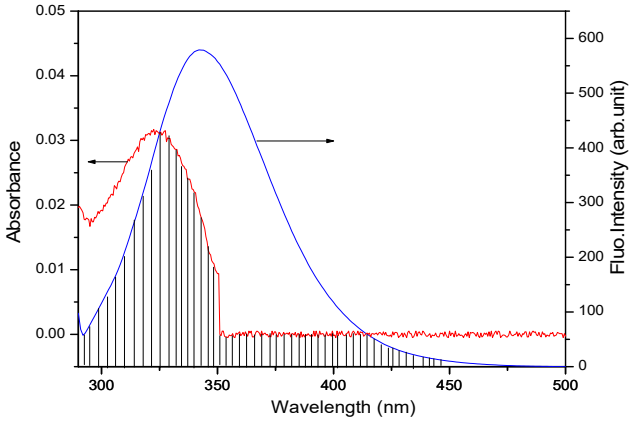

Fig. 5. 2HF's (2×10^{-6} M) absorption and BSA's (3×10^{-6} M) luminescence have spectral overlap (λ_{exc} = 280 nm).

Here, $N = 1.335$ and $\phi = 0.15$ [55-57]. Using Eqs. (6)-(8), $J = 3.508 \times 10^{-15}$ cm^3 M^{-1}, E = 0.477, R_0 = 2.14 nm, and $r = 2.18$ nm. The binding distance r, which ranges from $0.5R_0$ to $1.5R_0$, predicts a potential energy transfer from protein to medicine. The quenching method is static quenching, verified by the larger value of r than R_0 [58-65].

Identification of the Binding Site on BSA

The primary drug binding sites in protein molecules are situated in the subdomain IIA (site I) and IIIA (site II) although there are many other low-affinity binding sites [66,14]. To calculate the binding site, the competitive site binding experiments were conducted using the site binders warfarin and ibuprofen which can be bound particularly to site I and site II respectively [67,68]. The emission spectra of BSA (3×10^{-6} M) with different concentrations of 2HF in the

Table 3. Binding Constant of the 2HF-Protein Compound in the Presence of Site Markers at 298 K

System	K_a ($\times 10^4$ M^{-1})	n	R
BSA + 2HF	5.25	1.42	0.98
BSA + 2HF + Warfarin	4.45	0.90	0.99
BSA + 2HF + Ibuprofen	4.93	1.11	0.99

presence of warfarin (3×10^{-6} M) and ibuprofen (3×10^{-6} M), respectively were measured by exciting at 280 nm and at temperature 298 K. The spectra are shown in Fig. 6. The representative double logarithmic graph of the fluorescence quenching data is given in the inset of Figs. 6a and b. The binding constant (K_a) in the presence of warfarin and ibuprofen respectively are given in Table 3. The value of n is close to unity at all temperatures which is indicative of the availability of only one binding site of protein for ligand binding and is not affected by temperature [69]. It is observed that K_a significantly decreases in the presence of warfarin but the decrease is comparatively less in the presence of ibuprofen and quite close to the K_a of the BSA-2HF system. This clearly signifies the competitive binding of warfarin and 2HF with BSA. Thus, 2HF binds to the site I (subdomain IIA) of the serum albumin (BSA). This was further validated by the result of docking studies.

Analysis of Absorption Spectra

UV-Vis spectroscopy has been widely used to get information about the formation of a compound and explore any change in the protein structure [60,70,71]. The BSA (3×10^{-6} M) absorption spectra were scanned at different concentrations of 2HF between 200 nm and 450 nm. In the absorption spectra of flavonoids, the existence of two bands (Band I and Band II) is normally observed. Band I (300-400 nm) and Band II (240-280 nm) are due to the presence of the cinnamoyl moiety and benzoyl moiety, respectively [72]. However, 2HF does not show any significant absorption at 280 nm (see Fig. 7). Therefore, any change may be considered due to drug-protein interaction in the ground state. From Fig. 7, it is seen that the absorbance of serum albumin at 280 nm is enhanced with a gradual rise in the concentration of 2HF. This provides more evidence for the complexation in the ground state [73].

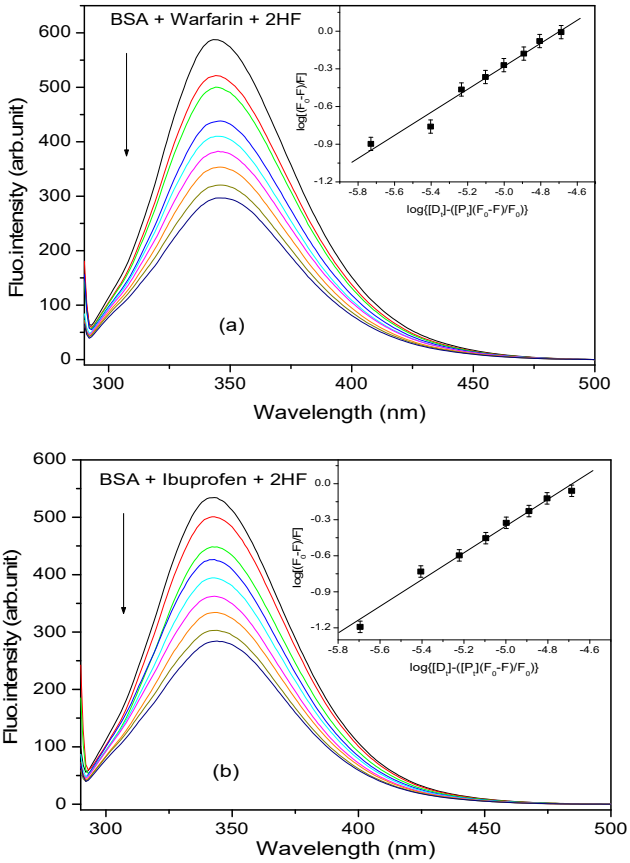

Fig. 6. Fluorescence profile of bovine serum albumin (3×10^{-6} M) with different concentrations of 2HF (0, 2.2, 4.4, 6.6, 8.8, 11, 13, 17, 22 $\times 10^{-6}$ M) in presence of (a) Warfarin (3×10^{-6} M) and (b) Ibuprofen (3×10^{-6} M) at 298 K. The matching plot of log[(F_0-F)/F] with log[Q]-([P](F_0-F)/F_0) is shown in the insets.

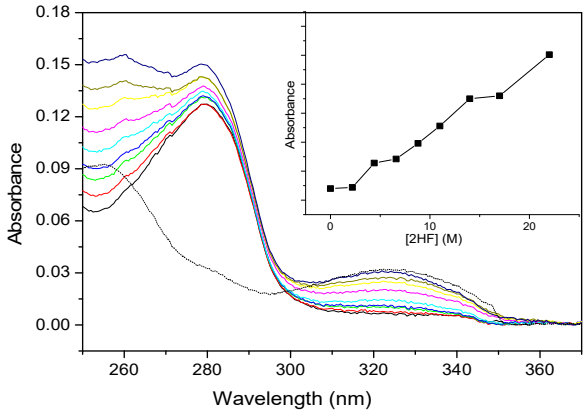

Fig. 7. Serum albumin's UV-visible spectra at varied 2HF concentrations. The UV-visible intensity fluctuation of BSA with [2HF] at 280 nm is displayed in the inset. dotted line is the absorption spectrum of 2HF (22 μM).

FT-IR Spectral Analysis

Fourier transform infrared (FTIR) spectroscopy was employed to study the structural changes of protein after interaction with the drug. According to Nandibewoor *et al.* [74], the infrared spectrum revealed that several amide bands made up the protein. The band at 1600-1700 cm^{-1} corresponds to amide I whereas the band at 1500-1600 cm^{-1} is due to amide II [59]. However, Amide I is commonly used to evaluate any change in protein secondary structure as it is more sensitive compared to amide II [75-77]. The infrared spectrum is shown in Fig. 8. Careful examination reveals that the presence of 2HF resulted in a 2 cm^{-1} change in the amide I peak. This implies that the association of BSA with 2HF caused a conformational change in the protein.

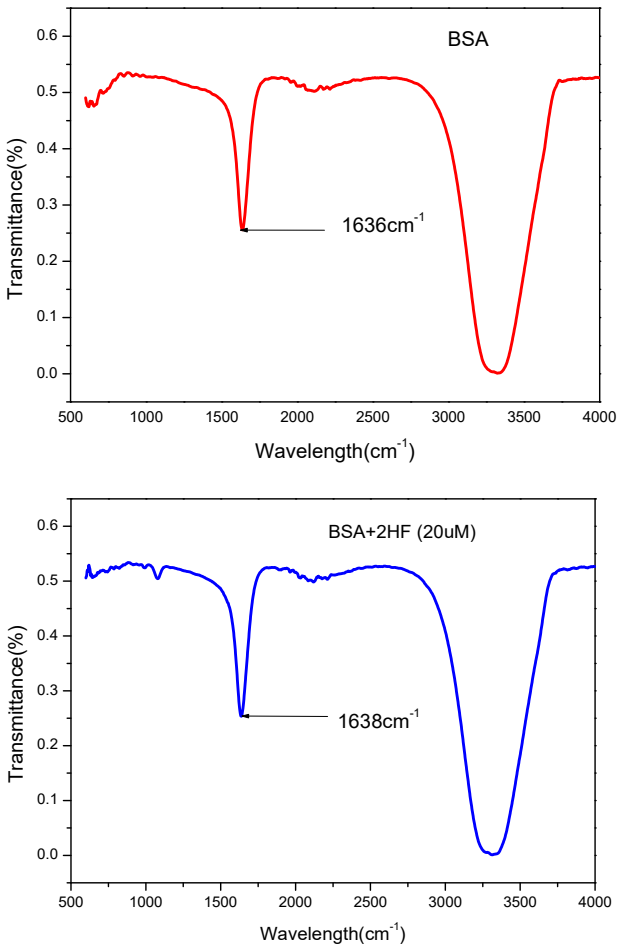

Fig. 8. FT-infra red spectra of (i) BSA and (ii) BSA in the presence of 2HF.

Circular Dichroism Studies

BSA has numerous selective chiral sites. Furthermore, The C2 carbon in the ring of 2HF is chiral. 2HF quenches the intrinsic fluorescence of BSA by altering the tryptophan lifetimes and this approach helps in studying the dynamics and structural changes in the microenvironment of proteins. Such studies thus aid in understanding the relationship between the chirality of BSA, its conformational alterations, and its biological functions [78].

To obtain information about the conformational change in BSA structure, CD measurement was done for BSA and BSA-2HF compound. The two distinct negative bands at approximately 208 nm and 222 nm in the CD spectra (Fig. 9) of free BSA and that associated with 2HF represent the structure of the α-helix structure of the serum albumin [79,80]. The subsequent decrease in both peaks upon the steady addition of 2HF suggests that the drug-protein association has resulted in some structural alterations in the protein structure. The result of CD is denoted in terms of mean residue ellipticity *[θ]* in $degcm^2\ dmol^{-1}$ (mdeg) and is expressed as

$$[\theta] = \frac{\theta_{obs}}{C_p nl \times 10} \tag{9}$$

Where, θ_{obs} = observed CD in milidegree, n = no. of amino acid residue (585), l mm = path length (0.1 cm), C_p = the molar amount of protein. The amount of α-helix present in bound and free serum albumin can be evaluated from the measured *[θ]* values at 208 nm by utilizing the Eq. (10) reported by Gao *et al.* [81].

$$\%\ of\ \alpha\ helix = \frac{[\theta]_{208} - 4000}{33000 - 4000} \times 100 \tag{10}$$

The calculated amount of % of α-helical in BSA and with two different concentrations of 2HF is 64.10%, 54.27%, and 48.61% in 3 × 10^{-6} M and 9 × 10^{-6} M, respectively. This decline in the α-helix percentage in the presence of the drug distinctly indicates that 2HF binds with BSA. Additionally, the similar spectra of protein (BSA) in the free and bound 2HF reveal the considerable presence of α-helical structure in BSA [82].

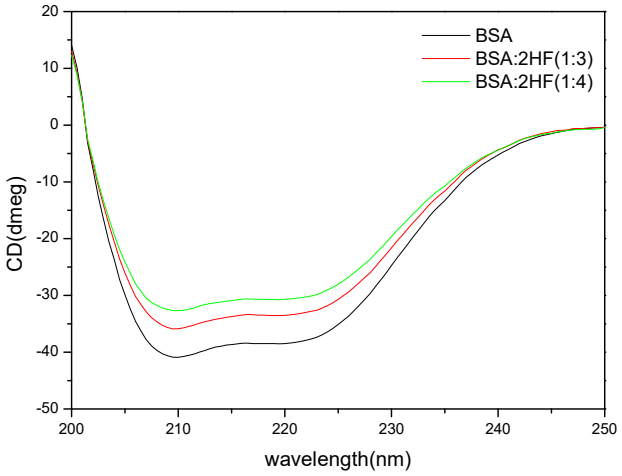

Fig. 9. CD spectra of free serum albumin and bound with 2HF.

Esterase-like Activity Studies

The impact of 2HF on the esterase-like activity of the protein was studied with different concentrations of PNPA as a substrate. The esterase-like activity of BSA was conducted at various concentrations of PNPA both in the free and bound 2HF by observing the optical density of the released product p-nitrophenol at wavelength 400 nm [23,25,83]. All the kinetic parameters like K_m and V_{max} were obtained from the Michalis-Menten (MM) plot as shown in Fig. 10a using Eq. (11) and K_{cat} was calculated using Eq. (12).

$$\upsilon_0 = \frac{V_{max}[S]}{K_m + [S]} \tag{11}$$

$$V_{max} = K_{cat}[E] \tag{12}$$

Where, υ_0, V_{max}, K_m, *[S]*, and *[E]* are the initial velocity, maximum velocity, Michaelis-Menten constant, the molar amount of PNPA, and total concentration of proteins, respectively. The initial velocities were evaluated from the slope of the graphs between 0-420 s [25,84,85]. The Lineweaver Burk plot was also plotted and shown in Fig. 10b. All the calculated values are listed in Table 4 for BSA. From the table, it can be noticed that K_m decreases with an increase in the concentration of 2HF, and V_{max} also changes in the presence of 2HF in BSA. This indicates that 2HF shows uncompetitive inhibition of the esterase-like activity of BSA [24,25,84]. The values of K_{cat}/K_m show that the catalytic efficiency of protein, for serum albumin increases the value with an increase in the concentration of 2HF. Further, the decrease in K_m and increase in the catalytic efficiency (K_{cat}/K_m) with increasing the concentration of 2HF indicates that the BSA undergoes a conformational change after binding with 2HF as observed in FT-IR and CD studies [23].

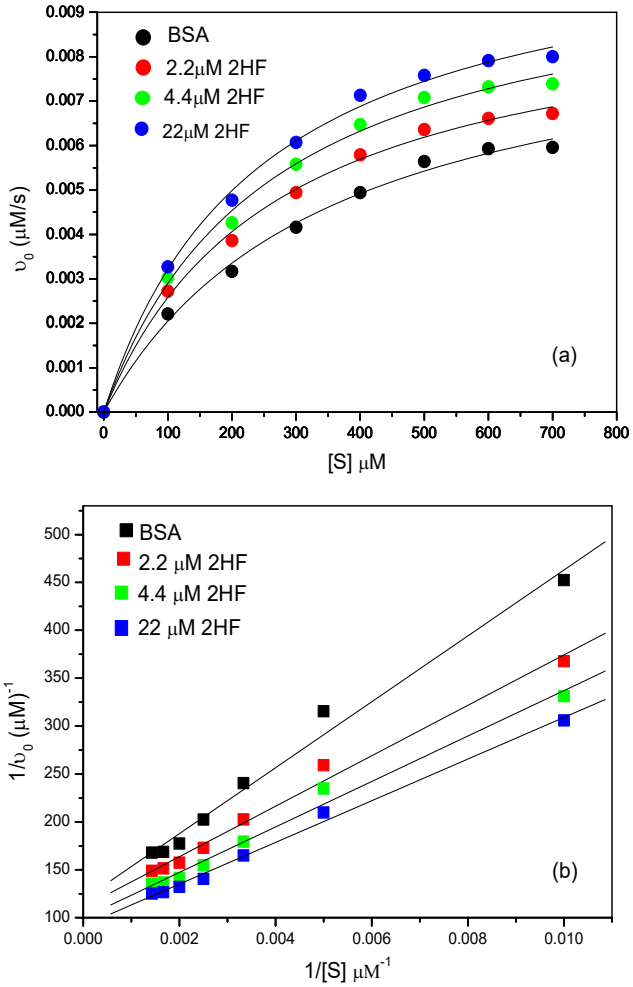

Fig. 10. (a) MM plot of BSA (3 μM) in the presence of 2HF (2.2, 4.4, and 22 μM) and (b) Lineweaver Burk plot of BSA (3 μM) in the presence of 2HF (2.2, 4.4, and 22 μM)

The above observation revealed the 2HF as an activator. The role of the activator in the whole phenomenon was discussed in the following five steps by a schematic diagram.

Table 4. MM kKinetic Parameters of Protein in the Presence of 2HF

System	K_m (μM)	V_{max} (× 10^{-2} μM^{-1} s^{-1})	K_{cat} (× 10^{-3} s^{-1})	K_{cat}/K_m (× 10^{-6} μM^{-1} s^{-1})
BSA	350.11 ± 43.82	0.92 ± 0.05	3.08	8.79
BSA + 2HF (2.2 μM)	268.30 ± 25.51	0.95 ± 0.03	3.17	11.82
BSA + 2HF (4.4 μM)	260.04 ± 28.09	1.04 ± 0.04	3.48	13.38
BSA + 2HF (22 μM)	244.93 ± 22.57	1.10 ± 0.04	3.70	15.09

Scheme I: The reaction between esterase (E) and phophorus ester XP

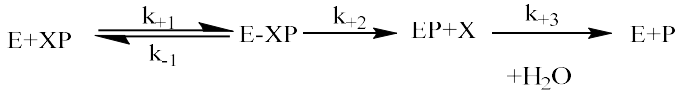

Scheme II: The reaction between Bovine Serum Albumin (Alb) and p-NPA

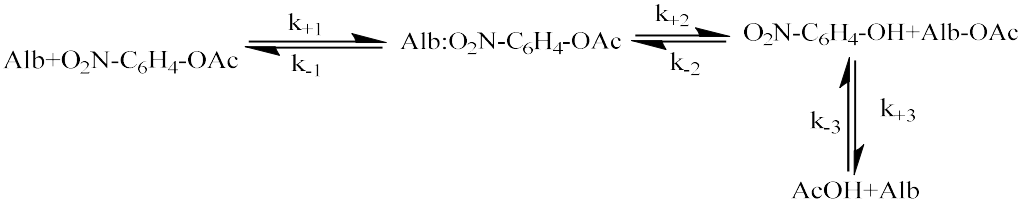

Scheme III: Spontaneous and albumin catalysed hydrolysis of phenylacetate. Here K_0 is the spontaneous hydrolysis constant,Ks is the substrate constant (dissociation constant of the enzyme-substrate complex), K_{cat} is the catalytic constant, k is the deacylation constant (dissociation constant of the acyl-albumin complex).

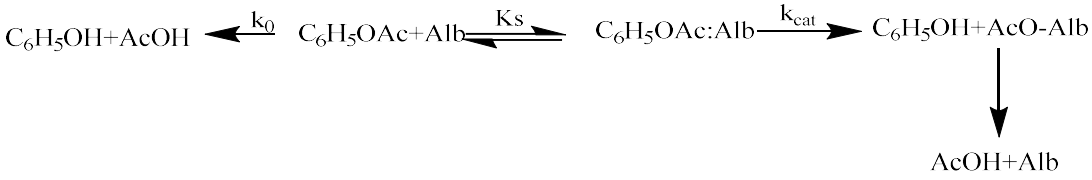

Scheme IV: Spontaneous and albumin catalyzed hydrolysis of 2'-hydroxyflavanone($C_{15}H_{12}O_3$), Here, K_h is the constant of spontaneous hydrolysis, Ka is the association constant of 2HF with Protein during the esterase activity, Kr= constant of albumin reactivation.

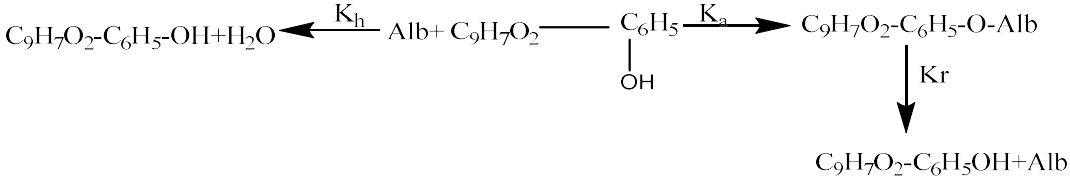

Scheme V: From (a-c) demonstrates all the main steps of interaction between acetylcholinesterase (E) and acetylproduct (S), and from (d-e), Where E is an enzyme(esterase), S is the substrate, P is the product.Kr is the constant of enzyme reactivation.

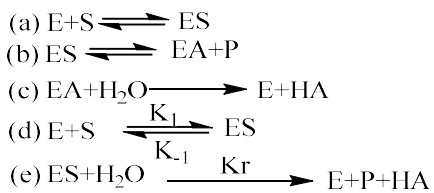

Molecular Docking Studies

To determine the preferred binding interaction between BSA and 2HF, molecular docking studies were implemented along with experimental studies which are summed up in Table 3. The docking outcomes indicate that 2HF preferably binds to site I in subdomain IIA of BSA as shown in Fig. 11 which is also in affirmation with site-marker experiments performed. The amino acid residues around 5Å from 2HF in site I of BSA as shown in (Fig. 11c) is VAL-215, LYS-211, ASP-323, ARG-208, LEU-326, ALA-212, GLY-327, GLU-353, PHE-329, LEU-330, LEU-346, ALA-349 [86]. The free binding energy (ΔG^0) was found to be -26.65 kJ mol^{-1} which is close to the experimental value (-26.72 kJ mol^{-1}). The slight difference in the value is due to the perfect or nearly perfect reaction conditions assumed in the theoretical calculation. The best-docked confirmation is displayed in Fig. 11a and the H-bonding between 2HF and amino acid residues of BSA (Fig. 11d) is found to be 1.936 Å (see Table 5). From the simulated results (Table 6), it is seen that $\Delta E_3 << \Delta E_2$ [87].

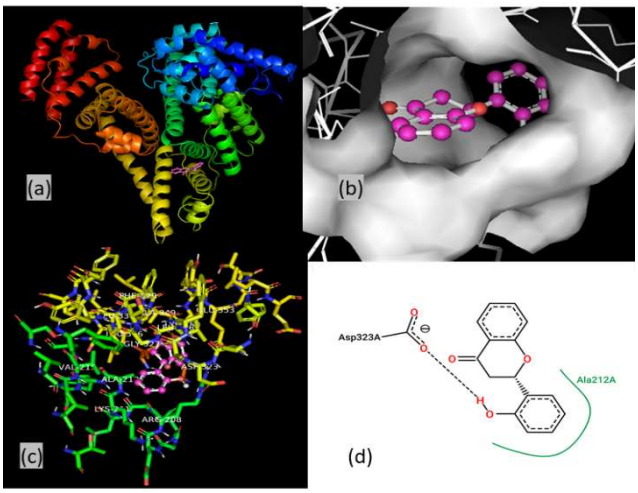

Fig. 11. 2HF-BSA association study using molecular docking. (a) The docked conformation with lowest $\Delta G°$ (b) 2HF inserted into the hydrophobic cavity in subdomain IIA of BSA (c) Serum albumin's amino acid residues around 5 Å of 2HF (d) 2D-diagram showing H- bonding interactions between 2HF and amino acid residues of serum albumin.

Effect of Metal Ions on the Binding of 2HF with BSA

Many bivalent metal ions have occurred in animals and the human body which can affect the binding of drugs with proteins and either enhance or reduce the effectiveness of the drug [54]. Therefore, we observe the association of ligand (2HF) with serum albumin (BSA) in some commonly occurring bivalent ions like Fe^{2+}, $Cu^{2+,}$ and Ca^{2+} respectively at 298 K. Figure 12 shows a decrease in the emission intensity of protein with the increase in the concentration of 2HF in presence of the 3 × 10^{-6} M metal ions respectively. Analysis of the quenching data with Eq. (3) is depicted in the insets of Figs. 12a, b, and c. The values that correspond to binding constants and binding sites are given in Table 7. It is found that although the number of binding sites is not affected, the binding constant between drug and proteins is found to

Table 5. Predicted Hydrogen Bond Formed between Atoms of BSA Amino Acid Residue and 2HF Obtained from Docking Results

BSA binding site	BSA atom	CHB atom	Distance (Å)
Site I (subdomain II A)	Asp-323: O	H	1.936

Table 6. Binding Interaction between Protein and Drug Ssimulated by Molecular Docking Method

Ligand	BindingSite in BSA	ΔG° (kJ mol^{-1})[a]	ΔE_1 (kJ mol^{-1})[b]	ΔE_2 (kJ mol^{-1})[c]	ΔE_3 (kJ mol^{-1})[d]
2HF	Site I (subdomain IIA)	-26.65	-29.16	-28.45	-0.67

[a]ΔG° is the binding energy change; [b]ΔE_1 is the interm6olecular interaction energy; [c]ΔE_2 is the sum of van der Waals energy, H-bonding energy, and desolvation free energy; [d]ΔE_3 is electrostatic energy.

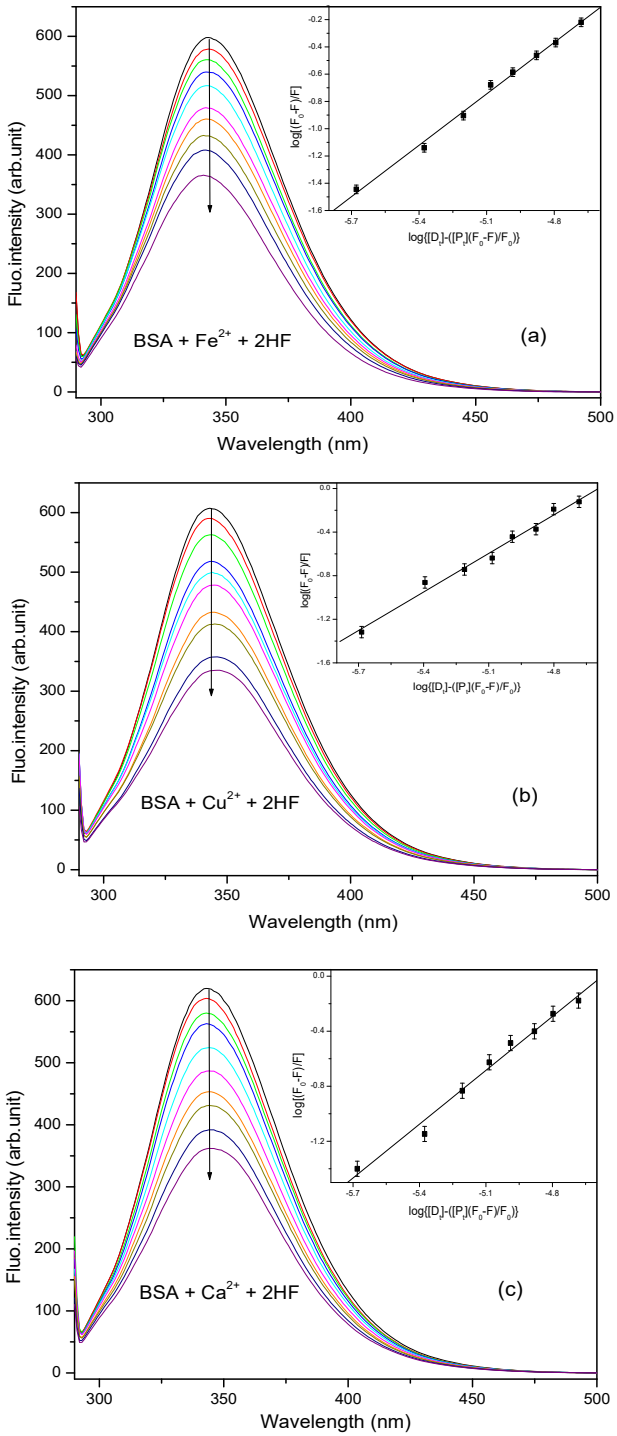

Fig. 12. Emission profile of serum albumin (3×10^{-6} M) at different concentrations of 2HF (0, 2.2, 4.4, 6.6, 8.8, 11, 14, 17, 22 ($\times 10^{-6}$ M) in presence of 3×10^{-6} M concentration of (a) Fe^{2+} (b) Cu^{2+} and (c) Ca^{2+} ions at 298 K. The related figure of log $[(F_0\text{-}F)/F]$ against $\log[Q]\text{-}([P](F_0\text{-}F)/F_0)$ is presented in the inset.

decrease significantly in the presence of the bivalent ions under study. This kind of observation is believed to be either due to the interaction of the metal with the drug in situ or because of the conformational change in BSA induced by the metal ions that reduce the binding affinity between 2HF and BSA [88]. The decrease in binding constant indicates that 2HF can be easily freed from blood [89,90] and lead to a decrease in the concentration of the drug in the blood. Therefore, it is required to regulate the dose limit of the 2HF to enhance the pharmacological effects of the drug as mentioned elsewhere [89-91].

Table 7. Binding Constant of the 2HF-Protein Compound in the Presence of Bivalent Ions at 298 K

System	K_a ($\times 10^4$ M^{-1})	n	R
BSA + 2HF	5.25 ± 0.50	1.52	0.98
BSA + 2HF + Fe^{2+}	3.21 ± 0.12	1.25	0.99
BSA + 2HF + Cu^{2+}	3.93 ± 0.11	1.17	0.99
BSA + 2HF + Ca^{2+}	3.76 ± 0.17	1.30	0.99

CONCLUSION

The association of BSA with 2′-hydroxyflavanone was investigated using spectroscopic along with molecular docking studies. The Stern-Volmer analysis of the quenching data obtained at five different temperatures indicates that the quenching mechanism of serum albumin with 2HF is static quenching. Förster distance r with $0.5R_0 < r < 1.5R_0$ also confirms the existence of static quenching. The higher value of k_q compared to the maximum bimolecular collisional quenching constant and the rise in the absorbance of BSA at wavelength 280 nm validates the BSA-2HF complex formation. The n value shows that there is only one site of BSA available for interaction. According to the competitive site binding assay, 2HF binds to BSA subdomain IIA. The outcomes of molecular docking serve as additional confirmation of this. The thermodynamic parameters signify that the 2HF-BSA complexation is spontaneous and involves binding forces such as van der Waal's force and H-bonding interaction. Enthalpy was mainly found to be the driving

force. FTIR study revealed the conformational change in BSA after interacting with 2HF. This is further supported by the quantitative analysis of circular dichroism results. In addition to the conformational change in protein structure after binding with 2HF, the esterase-like activity study of BSA shows an increase in the catalytic activity of BSA with an increase in 2HF concentration. The binding constant decreases in the presence of bivalent metallic ions indicating that 2HF binds to protein less efficiently and reduces its availability in the blood. This observation presents a structural understanding of anticancer properties containing the drug 2HF. The information gathered in this study will be crucial in understanding the effect and action of the drug and in designing new drugs with improved efficiency of its specific action.

ACKNOWLEDGMENT

One of the authors thanks the National Institute of Technology Silchar, Assam, India, for the financial support. Special thanks to Abhijit Shyam and Amit Kumar Pradhan from Assam University, Silchar for their valuable assistance in docking. The authors acknowledge the Advance Material Research Centre, IIT Mandi, Himachal Pradesh for providing Circular Dichroism measurement.

REFERENCES

[1] Bosetti, C.; Rossi, M.; McLaughlin, J. K; *et al.*, Flavonoids and the Risk of Renal Cell Carcinoma. *Cancer Epidemiol. Biomarkers Prev.* **2007**, *16* (1), 98-103, DOI: 10.1158/1055-9965.EPI-06-0769.

[2] Bertoia, M.; Albanes, D.; Mayne, S. T.; Mannisto, S.; Virtamo, J.; Wright, E. M., No Association between Fruit, Vegetables, Antioxidant Nutrients and Risk of Renal Cell Carcinoma. *Int. J. Canc.* **2010**, *126*, 1504-1512, DOI: 10.1002/ijc.24829.

[3] Amin, R. A. R. M.; Kucuk, O.; Khuri, F. R.; Shin, D. M., Perspectives for Cancer Prevention with Natural Compounds. *J. Clin. Oncol.* **2009**, *27* (16), 2712-2725, DOI: 10.1200/JCO.2008.20.6235.

[4] Khan, M. K.; Huma, Z. -E.; Dangles, O. A., Comprehensive Review on flavanones, the major Citrus Polyphenols. *J. Food Compos. Anal.* **2014**, *33* (1), 85-104, DOI: 10.1093/synbio/ysaa012.

[5] Shen, S. -C.; Ko, C. H.; Tseng, S. -W.; Tsai, S. -H.; Chen, Y. -C., Structurally related antitumor effects of flavanones in vitro and in vivo: involvement of caspase 3 activation, p21 gene expression, and reactive oxygen species production. *Toxicol. Appl. Pharmacol.* **2004**, *197* (2), 84-95, DOI: 10.1016/j.taap.2004.02.002.

[6] Singhal, S. S.; Singhal, J.; Figarola, L. J.; Riggs, A.; Horne, D.; Awasthi, S., 2′-Hydroxyflavanone: A Promising Molecule for Kidney Cancer Prevention. *Biochem. Pharmacol*. **2015**, *96* (1), 151-158, DOI: 10.1016/j.bcp.2015.04.022.

[7] Shin, S. Y.; Kim, J. H.; Lee, J. H.; Lim, Y.; Lee, Y. H., 2-Hydroxyflavanone Induces Apoptosis through Egr-1 Involving Expression of Bax, p21, and NAG-1 in Colon Cancer Cells. *Mol. Nutr. Food Res*. **2012**, *56*, 761-774, DOI: 10.1002/mnfr.201100651.

[8] Hsiao, Y. C.; Kuo, W. -H.; Chen, P. -N.; *et al*., Flavanone and 2′-OH Flavanone Inhibit Metastasis of Lung Cancer Cells *via* Down-Regulation of Proteinases Activities and MAPK pathway. *Chem. Biol. Interact.* **2007**, *167* (3), 193-206, DOI: 10.1016/j.cbi.2007.02.012.

[9] Hsiao, Y. C.; Hseih, Y. S.; Kuo, W. H.; *et al.*, The tumor-growth inhibitory activity of flavanone and 2¢-OH flavanonein vitro and in vivo through induction of cell cycle arrest and suppression of cyclins and CDKs. *J. Bio. Medi. Sci.* **2007**, *14*, 107-119, DOI: 10.1007/s11373-006-9117-3.

[10] Nagaprashantha, L. D.; Vatsyayan, R.; Singhal, J.; *et al.,* 2′-Hydroxyflavanone Inhibits Proliferation, Tumor Vascularization and Promotes Normal Differentiation in VHL -mutant Renal Cell Carcinoma. *Carcinogenesis* **2011***, 32* (4)*,* 568-575*,* DOI: 10.1093/carcin/bgr021.

[11] Singhal, J.; Nagaprashantha, L.; Chikaral, S.; Awasthi, S.; Horne, D.; Singhal, S. S., 2'-Hydroxyflavanone: A novel strategy for targeting breast cancer. *Oncotarget* **2017**, *8* (43), 75025-75037, DOI: 10.18632/oncotarget.20499.

[12] Xiao, J.; Cao, H.; Wang, Y.; Yamamoto, K.; Wei, X., Structure-affinity relationship of flavones on binding to serum albumins: Effect of hydroxyl groups on ring A. *Mol. Nutr. Food Res.* **2010**, *54*, S253-S260,

DOI: 10.1002/mnfr.200900454.

[13] Roy, A. S.; Dinda, A. K.; Pandey, N. K.; Dasgupta, S., Effects of Urea, Metal ions and Surfactants on the Binding of Baicalein with Bovine Serum Albumin. *J. Pharm. Anal*. **2016**, *6* (4), 256-267, DOI: 10.1016/j.jpha.2016.04.001.

[14] Rabbani, G.; Ahn, S. N., Review: Roles of human serum albumin in prediction, diagnoses and treatment of COVID-19. *Int. J. Biol. Macromol.* **2021**, *193*, 948-955, DOI: 10.1016/j.ijbiomac.2021.10.095.

[15] Peters, T., Serum Albumin. *Adv. Protein Chem.* **1985**, *37*, 161-245, DOI: 10.1016/S0065-3233(08)60065-0.

[16] Michnik, A.; Michalik, K.; Kluczewska, A.; Drzazga, Z., Comparative DSC Study of Human and Bovine Serum Albumin. *J. Therm. Anal. Calorim.* **2006**, *84* (1), 113-117, DOI: 10.1007/s10973-005-7170-1.

[17] Shi, J. -H.; Pan, D. -Q.; Wang, X. -X.; Liu, T. -T.; Jiang, M.; Wang, Q., Characterizing the Binding Interaction between Antimalarial Artemether (AMT) and Bovine Serum Albumin (BSA): Spectroscopic and molecular docking methods. *J. Photochem. Photobiol. B: Biol.* **2016**, *162*, 14-23, DOI: 10.1016/j.jphotobiol.2016.06.025

[18] Karthikeyan, S.; Bharanidharan, G.; Kesherwani, M.; *et al*., Insights into the Binding of Thiosemicarbazone Derivatives with Human Serum Albumin: Spectroscopy and Molecular Modelling Studies. *J. Biomol. Struct. Dyn*. **2016**, *34* (6), 1264-1281, DOI: 10.1080/07391102.2015.1075905

[19] Wani, T. A.; AlRabiah, H.; Bakheit, A. H.; Kalam, M. A.; Zargar, S., Study of binding interaction of rivaroxaban with bovine serum albumin using multi-spectroscopic and molecular docking approach. *Chem. Cent. J.* **2017**, *11* (1), 134-142, DOI: 10.1186/s13065-017-0366-1

[20] Suryawanshi, V. D.; Walekar, L. S.; Gore, A. H.; Anbhule, P. V.; Kolekar, G. B., Spectroscopic Analysis on the Binding Interaction of Biologically Active Pyrimidine Derivative with Bovine Serum Albumin. *J. Pharm. Anal.* **2016**, *6* (1), 56-63, DOI: 10.1016/j.jpha.2015.07.001

[21] Islam, M. M.; Sonu, V. K.; Gashinga, P. M.; Moyon, N. S.; Mitra, S., Caffeine and Sulfadiazine Interact Differently with Human Serum Albumin: A Combined Fluorescence and Molecular Docking Study. *Spectrochim. Acta A: Mol. Biomol. Spectrosc.* **2016**, *152*, 23-33, DOI: 10.1016/j.saa.2015.07.051.

[22] Khalili, L.; Dehghan, G., A Comparative Spectroscopic, Surface Plasmon Resonance, Atomic Force Microscopy and Molecular Docking Studies on the Interaction of Plant Derived Conferone with Serum Albumins. *J. Lumin.* **2019**, *211*, 193-202, DOI: 10.1016/j.jlumin.2019.03.048

[23] Patel, R.; Maurya, N.; Parray, M. U. D.; *et al.,* Esterase activity and conformational changes of bovine serum albumin toward interaction with mephedrone: Spectroscopic and computational studies. *J Mol Recognit.* **2018**, *31* (11), e2734-e2746, DOI: 10.1002/jmr.2734

[24] Chandel, T. I.; Rabbani, G.; Khan, M. V.; *et al*., Binding of anti-cardiovascular drug to serum albumin: An insight in the light of spectroscopic and computational approaches. *J. Biomol. Struct. Dyn.* **2018**, *36* (1), 54-67, DOI: 10.1080/07391102.2016.1266968.

[25] Patel, R.; Singh, B.; Sharma, A.; *et al*., Interaction and esterase activity of albumin serums with orphenadrine: A spectroscopic and computational approach. *J. Mol. Struct*. **2021**, *1239*, 30522-130532, DOI: 10.1016/j.molstruc.2021.130522

[26] Morris, G. M.; Goodsell, D. S.; Halliday, R. S.; *et al.,* AutoDock, Version 4.0.1. *The Scripps Research Institute. La Jolla* **2007**.

[27] Frisch, M. J.; Trucks, G. W.; Schlegel, H. B.; Scuseria, G. E.; Robb, M. A.; Cheeseman, J. R.; *et al*., In, Gaussian, Inc. Gaussian09, revision a.02. *Wallingford CT, USA* **2009**.

[28] Zhao, Y.; Truhlar, D. G., Density Functionals with Broad Applicability in Chemistry. *Acc. Chem. Res.* **2008**, *41* (2), 157-167, DOI: 10.1021/ar700111a.

[29] Gasteiger, J.; Marsili, M., Iterative partial equalization of orbital electronegativity-a rapid access to atomic charges. *Tetrahedron* **1980**, *36*, 3219-3228, DOI: 10.1016/0040-4020(80)80168-2.

[30] Tiwari, R.; Mahasenan, K.; Pavlovicz, R.; Li, C.; Tjarks, W., Carborane clusters in computational drug design: a comparative docking evaluation using AutoDock, FlexX, Glide, and Surflex. *J. Chem. Inf. Model* **2009**, *49*, 1581-1589, DOI: 10.1021/ci900031y.

[31] Tietze, S.; Strassnig, C.; Tietze. S.; *et al*., Improved Cyclodextrin-Based Receptors for Camptothecin by Inverse Virtual Screening**.** *Chem. Eur. J.* **2007**, *13*, 6801-6809, DOI: 10.1002/chem.200700661.

[32] Takeda, K.; Wada, A.; Yamamoto, K.; Yoshiko, M.; Aoki, K., Conformational Change of Bovine Serum Albumin by Heat Treatment. *J. Protein Chem.*, **1989**, *8* (5), 653-659. https://doi.org/10.1007/BF01025605.

[33] Chaves, O.A.; Da Silva, V.A.; Sant'Anna, C.M.R.; et al., Binding Studies of Lophirone B with Bovine Serum Albumin (BSA): Combination of Spectroscopic and Molecular Docking Techniques. *J. Mol. Struct.* **2017**, 1128, 606-611, DOI: 10.1016/j.molstruc.2016.09.036

[34] Rabbani, G.; Baig, Md. H.; Jan, A.T.; et.al., Binding of erucic acid with human serum albumin using a spectroscopic and molecular docking study. *Int. J. Biol. Macromol.* **2017**, *105* (3), 1572-1580, DOI: 10.1016/j.ijbiomac.2017.04.051

[35] Rabbani, G.; Khan, Md. J.; Ahmad, A.; Maskat, Md. Y.; Khan, R.H., Effect of copper oxide nanoparticles on the conformation and activity of galactosidase. *Colloids Surf. B: Biointerfaces* **2014**, 123, 96-105, DOI: 10.1016/j.colsurfb.2014.08.035

[36] Lakowicz, J. R., Principles of fluorescence spectroscopy, 3rd edn. *Springer science + business media, NY, USA* **2006**.

[37] Rabbani, G.; Lee, E. J.; Ahmad K.; Baig, Md. H.; Choi, I., Binding of Tolperisone Hydrochloride with Human Serum Albumin: Effects on the Conformation, Thermodynamics, and Activity of HSA. *Mol. Pharm.* 2018, *15* (4), 1445-1456, DOI: 10.1021/ acs.molpharmaceut.7b00976

[38] Lakowicz, J. R.; Weber, G., Quenching of fluorescence by oxygen. A Probe for Structural Fluctuations in Macromolecules. *Biochemistry* **1973**, *12* (21), 4161-4170, DOI: 10.1021/bi00745a020.

[39] Ware, W.R., Oxygen Quenching of Fluorescence in Solution: An Experimental Study of the Diffusion Process. *J. Phys. Chem.* **1962**, *66* (3), 455-458, DOI: 10.1021/j100809a020.

[40] Yan, X.; Liu, B.; Chong, B.; Cao, S., Interaction of Cefpiramide Sodium with Bovine Hemoglobin and Effect of the Coexistent Metal ion on the Protein-Drug Association. *J. Lumin.* **2013**, *142*, 155-162, DOI: 10.1016/j.jlumin.2013.04.009.

[41] Mandal, P.; Ganguly, T., Fluorescence Spectroscopic Characterization of the Interaction of Human Adult Hemoglobin and Two Isatins, 1-Methylisatin and 1-Phenylisatin: A Comparative Study. *J. Phys. Chem. B* **2009**, *113* (45), 14904-14913, DOI: 10.1021/ jp9062115.

[42] Wang, Y. -Q.; Zhang, H. -M.; Zhang, G. -C.; Tao, W. -H.; Tang, S. -H., Interaction of the Flavonoid Hesperidin with Bovine Serum Albumin: A Fluorescence Quenching Study. *J. Lumin.* **2007**, *126* (1), 211-218, DOI: 10.1016/j.jlumin.2006.06.013.

[43] Zhang, Q.; Ni, Y., Comparative Studies on the Interaction of Nitrofuran Antibiotics with Bovine Serum Albumin. *RSC Adv.* **2017**, *7*, 39833-39841, DOI: 10.1039/ C7RA05570F.

[44] Xu, H.; Liu, Q.; Zuo, Y.; Bi, Y.; Gao, S., Spectroscopic Studies on the Interaction of Vitamin C with Bovine Serum Albumin. *J Solution Chem.* **2009**, *38*, 15-25. DOI: 10.1007/s10953-008-9351-6.

[45] Soori, H.; Rabbani-Chadegani, A.; Davoodi, J., Exploring binding affinity of oxaliplatin and carboplatin, to nucleoprotein structure of chromatin: Spectroscopic study and histone proteins as a target. *European Journal of Medicinal Chemistry*, **2015**, *89*, 844-850. https://doi.org/10.1016/j.ejmech.2014.10.063.

[46] Dufour, C.; Dangles, O., Flavonoid-serum albumin complexation: determination of binding constants and binding sites by fluorescence spectroscopy. *Biochimica et Biophysica Acta*, **2005**, *1721*, 164-173. DOI: 10.1016/j.bbagen.2004.10.013.

[47] Musteata, M. F., Ligand-Receptor Binding and Determination of Free Concentrations, Handbook of Solid Phase Microextraction. *Department of Pharmaceutical Sciences*, Albany College of Pharmacy and Health Sciences, Albany, NY, USA, **2005**. DOI: 10.1016/B978-0-12-416017-0.00011-5.

[48] Hosseinzadeh, M.; Nikjoo, S.; Zare, N. *et al.* Characterization of the structural changes of human serum albumin upon interaction with single-walled and multi-walled carbon nanotubes: spectroscopic and molecular modelling approaches. *Res Chem Intermed*.

2019, *45*, 401-423. https://doi.org/10.1007/s11164-018-3608-5

[49] Malek-Esfandiari, Z.; Rezvani-Noghani, A.; Sohrabi, T.; Mokaberi, P.; Amiri-Tehranizadeh, Z.; Chamani, J., Molecular Dynamics and Multi-Spectroscopic of the Interaction Behavior between Bladder Cancer Cells and Calf Thymus DNA with Rebeccamycin: Apoptosis through the Down Regulation of PI3K/AKT Signaling Pathway. *Journal of fluorescence*, **2023**, *33* (4), 1537-1557. https://doi.org/10.1007/s10895-023-03169-4.

[50] Ross, P. D.; Subramanian, S., Thermodynamics of Protein Association Reactions: Forces Contributing to Stability. *Biochemistry* **1981**, *20* (11), 3096-3102, DOI: 10.1021/bi00514a017.

[51] Esfahian, A. J.; Azar, V. P.; Sajedi, S., Interaction of Glutathione with Bovine Serum Albumin: Spectroscopy and Molecular Docking. *Food Chem.* **2016**, *202*, 426-431, DOI: 10.1016/j.foodchem.2016.02.026.

[52] Mohammadzadeh-Aghdash, H.; Dolatabadi, N. E. J.; Dehghan, P.; Panahi-Azar, V.; Barzegar, A., Multi-spectroscopic and molecular modeling studies of bovine serum albumin interaction with sodium acetate food additive. *Food chem*. **2017,** *228*, 265-269. https://doi.org/10.1016/j.foodchem.2017.01.149.

[53] Rabbani, G.; Ahmad, E.; Khan, M. V.; Ashraf, Md. T.; Bhat, R.; Khan, R. H., Impact of structural stability of cold adapted Candida antarctica lipase B (CaLB): in relation to pH, chemical and thermal denaturation. *RSC Adv.* **2015,** *5*, 20115-20131, DOI: 10.1039/C4RA17093H.

[54] Rabbani, G.; Ahmad, E.; Zaidi, N.; Khan, R. H., pH-Dependent Conformational Transitions in Conalbumin (Ovotransferrin), a Metalloproteinase from Hen Egg White. *Cell Biochem. Biophys.* **2011**, *61*, 551-560, DOI: 10.1007/s12013-011-9237-x.

[55] Rahman, S.; Rehman, Md. T.; Rabbani, G.; *et al*., Insight of the Interaction between 2,4-thiazolidinedione and Human Serum Albumin: A Spectroscopic, Thermodynamic and Molecular Docking Study. *Int. J. Mol. Sci.* ***2019****, 20* (11), 2727-2745, DOI: 10.3390/ijms20112727.

[56] Dolatabadi, N. E. J.; Panahi-Azar, V.; Barzegar, A.; Jamali, A.A.; Kheirdoosh, F.; Kashanian, S.; Omidi, Y., Spectroscopic and molecular modeling studies of human serum albumin interaction with propyl gallate. *RSC Adv*. **2014**, *4* (110), 64559-64564. DOI: 10.1039/C4RA11103F.

[57] Fathi, F.; Dolatabadi, N. E. J.; Rashidi, R. M.; Omidi, Y., Kinetic studies of bovine serum albumin interaction with PG and TBHQ using surface plasmon resonance. *Int. J. Biol. Macromol*. **2016**, *91*, 1045-1050. https://doi.org/10.1016/j.ijbiomac.2016.06.054.

[58] Shi, J. H.; Pan, D. Q.; Jiang, M.; Liu, T. T.; Wang, Q., Binding Interaction of Ramipril with Bovine Serum Albumin (BSA): Insights from Multi-Spectroscopy and Molecular Docking Methods. *J. Photochem. Photobiol. B: Biol.* **2016**, *164*, 103-111, DOI: 10.1016/j.jphotobiol.2016.09.025.

[59] Rabbani, G.; Baig, Md. H.; Lee, E. J.; Cho, W. -K.; Ma, J. Y.; Choi, I., Biophysical Study on the Interaction between Eperisone Hydrochloride and Human Serum Albumin Using Spectroscopic, Calorimetric, and Molecular Docking Analyses. *Mol. Pharm.* **2017**, *14* (5), 1656-1665, DOI: 10.1021/acs.molpharmaceut.6b01124.

[60] Abdullah, S. M. S.; Fatma, S.; Rabbani, G.; Ashraf, J. M., A Spectroscopic and molecular docking approach on the binding of tinzaparin sodium with human serum albumin. *J. Mol. Struct.* **2017**, *1127*, 283-288, DOI: 10.1016/j.molstruc.2016.07.108.

[61] Ishtikhar, Md.; Rabbani, G.; Khan, H. R., Interaction of 5-fluoro-5′-deoxyuridine with human serum albumin under physiological and non-physiological condition: A biophysical investigation. *Colloids Surf. B: Biointerfaces* **2014**, *123*, 469-477, DOI: 10.1016/j.colsurfb.2014.09.044.

[62] Singh, T. S.; Mitra, S., Interaction of cinnamic acid derivatives with serum albumins: A fluorescence spectroscopic study. *Spectrochim. Acta A Mol. Biomol. Spectrosc.* **2011**, *78* (3), 942-948, DOI: 10.1016/j.saa.2010.11.046

[63] Cyril, L.; Earl, J. K.; Sperry, W. M., Press. Biochemist's handbook, London. *E& FN Epon Led, UK* **1961**.

[64] Cheng, Z. -J.; Zhao, H. -M.; Xu, Q. -Y.; Liu, R., Investigation of the Interaction between Indigotin and Two Serum Albumins by Spectroscopic Approaches. *J.*

Pharm. Anal. **2013**, *3* (4), 257-269, DOI: 10.1016/j.jpha.2013.01.004.

[65] Zhang, Y. -Z.; Dai, J.; Xiang, X.; Li, W. -W.; Liu, Y., Studies on the Interaction between Benzidine and Bovine Serum Albumin by Spectroscopic Methods. *Mol. Biol. Rep.* **2010**, *37*, 1541-1549, DOI 10.1007/s11033-009-9555-x.

[66] Rabbani, G.; Ahn, S. N., Structure, enzymatic activities, glycation and therapeutic potential of human serum albumin: A natural cargo. *Int. J. Biol. Macromol.* **2019**, *123*, 979-990, DOI: 10.1016/j.ijbiomac.2018.11.053.

[67] Singh, S. K.; Kishore, N., Thermodynamic Insights into the Binding of Triton X-100 to Globular Proteins: A Calorimetric and Spectroscopic Investigation. *J. Phys. Chem. B* **2006**, *110* (19), 9728-9737, DOI: 10.1021/jp0608426.

[68] Sudlow, G.; Birkett, D. J.; Wade, D. N., The Characterization of Two Specific Drug Binding Sites on Human Serum Albumin. *Mol. Pharmacol.* **1975**, *11* (6), 824-832, DOI: content/11/6/824.

[69] Ishtikhar, Md.; Rabbani, G.; Khan, S.; Khan, H. R., Biophysical investigation of thymoquinone binding to 'N' and 'B' isoform of human serum albumin and explore the interaction mechanism and radical scavenging activity. *RSC Adv.* **2015**, *5* (24), 18218-18232, DOI: 10.1039/C4RA09892G.

[70] Rabbani, G.; Ahmad, E.; Zaidi, N.; Fatima, S.; Khan, R. H., pH-Induced Molten Globule State of Rhizopus niveus Lipase is More Resistant Against Thermal and Chemical Denaturation Than Its Native State. *Cell Biochem. Biophys.* **2012**, *62*, 487-499, DOI: 10.1007/s12013-011-9335-9.

[71] Rabbani, G.; Kaur, J.; Ahmad, E.; Khan, R. H.; Jain, S. K., Structural characteristics of thermostable immunogenic outer membrane protein from Salmonella enterica serovar Typhi. *Appl. Microbiol. Biotechnol*. **2014**, *98*, 2533-2543, DOI: 10.1007/s00253-013-5123-3.

[72] Mabry, T. J.; Markham, K. R.; Thomas, M. B., The Ultraviolet Spectra of Flavones and Flavonols. The Systematic Identification of Flavonoids. *Springer, Berlin, Heidelberg* **1970**, 165-226, DOI: 10.1007/978-3-642-88458-0_6.

[73] Wani, T. A.; Bakheit, A. H.; Abounassif, M. A.; Zargar, S., Study of Interactions of an Anticancer Drug Neratinib with Bovine Serum Albumin: Spectroscopic and Molecular Docking Approach. *Front. Chem.* **2018**, *6*, 47-56, DOI: 10.3389/fchem.2018.00047.

[74] Naik, K. M.; Nandibewoor, S. T., Spectroscopic studies on the interaction between chalcone and bovine serum albumin. *J. Lumin.* **2013**, *143*, 484-491, DOI: 10.1016/j.jlumin.2013.05.013.

[75] Lin, S. Y.; Wei, Y. S.; Li, M. J.; Wang, S. L., Effect of ethanol or/and captopril on the secondary structure of human serum albumin before and after protein binding. *Eur. J. Pharm. Biopharm.* **2004**, *57*, 457-464, DOI: 10.1016/j.ejpb.2004.02.005.

[76] Brauner, J. W.; Flach, C. R.; Mendelsohn, R., A quantitative reconstruction of the amide I contour in the IR spectra of globular proteins: from structure to spectrum. *J. Am. Chem. Soc.* **2005***, 127*, 100-109, DOI: 10.1021/ja0400685

[77] Rahmelow, K.; Hubner, W., Secondary structure determination of proteins in aqueous solution by infrared spectroscopy: A comparison of multivariate data analysis methods. *Anal. Biochem.* **1996**, *241*, 5-13, DOI: 10.1006/abio.1996.0369.

[78] Wei, Y.; Dong, C.; Liu, D.; Shuang, S.; Huie, C. W., Enantioselective quenching of room-temperature phosphorescence lifetimes of proteins: bovine and human serum albumins. *Biomacromolecules*, **2007**, *8*(3), 761–764. https://doi.org/10.1021/bm061012.

[79] Zhou, Q.; Xiang, J.; Tang, Y.; *et al*., Investigation on the interaction between a heterocyclic aminal derivative, SBDC, and human serum albumin. *Colloids Surf. B Biointerfaces* **2008**, *61*, 75-80, DOI: 10.1016/j.colsurfb.2007.07.007.

[80] Sun, Z.; Xu, H.; Cao, Y.; Wang, F.; Mi, W., Elucidating the interaction of propofol and serum albumin by spectroscopic and docking methods. *J. Mol. Liq.* **2016**, *219*, 405-410, DOI: 10.1016/j.molliq.2016.03.040.

[81] Gao, H.; Lei, L.; Liu, J.; Kong, Q.; Chen, X.; Hu, Z., The study on the interaction between human serum albumin and a new reagent with antitumour activity by spectrophotometric methods. *J. Photochem. Photobiol. A: Chemistry* **2004**, *167*, 213-221, DOI: 10.1016/j.jphotochem.2004.05.017.

[82] Sugio, S.; Kashima, A.; Mochizuki, S.; Noda, M.; Kobayashi, K., Crystal structure of human serum albumin at 2.5 °A resolution. *Protein Eng*. **1999**, *12*, 439-446, DOI: 10.1093/protein/12.6.439.

[83] Dohare, N.; Siddiquee, Md. A.; Parray, M. U. D; Kumar, A.; Patel, R., Esterase activity and interaction of human hemoglobin with diclofenac sodium: A spectroscopic and molecular docking study. *J. Mol. Recognit.* **2020**, *33* (8), e2841-e2851, DOI: 10.1002/jmr.2841.

[84] Moradi, N.; Ashrafi-Kooshk, Md. R; Ghobadi, S; Shahlaei, M.; Khodarahmi, R., Spectroscopic study of drug-binding characteristics of unmodified and pNPA-based acetylated human serum albumin: Do esesterase activity affect microenvironment of drug binding sites on the protein? *J. Lumin*. **2015**, *160*, 351-361, DOI: 10.1016/j.jlumin.2014.11.019.

[85] Maurya, N.; Maurya, K. J.; Singh, K. U.; Dohare, R.; Zafaryab, Md., Rizvi, A. M. M.; Kumari, M.; Patel, R., *In Vitro* Cytotoxicity and Interaction of Noscapine with Human Serum Albumin: Effect on Structure and Esterase Activity of HSA. *Mol. Pharmaceutics* **2019**, *16*, 952-966, DOI: 10.1021/ acs.molpharmaceut.8b00864

[86] Ahmad, E.; Rabbani, G.; Zaidi, N.; *et al*., Stereo-Selectivity of Human Serum Albumin to Enantiomeric and Isoelectronic Pollutants Dissected by Spectroscopy, Calorimetry and Bioinformatics. *PloS One* **2011**, *6* (11), e26186-e26203, DOI: 10.1371/journal.pone.0026186.

[87] Varshney, A.; Rehan, M.; Subbarao, N.; Rabbani, G.; Khan, R. H., Elimination of Endogenous Toxin, Creatinine from Blood Plasma Depends on Albumin Conformation: Site Specific Uremic Toxicity & Impaired Drug Binding. *PLoS One* **2011**, *6* (2), e17230-e17244, DOI: 10.1371/journal.pone.0017230.

[88] Roy, A. S.; Dinda, A. K.; Chaudhury, S.; Dasgupta, S.; Binding of antioxidant flavonol morin to the native state of bovine serum albumin: Effects of urea and metal ions on the binding. *J. Lumin.* **2014**, *145*, 741-751, DOI: 10.1016/j.jlumin.2013.08.054.

[89] Yang, Y.; Li, D.; Xu, C., Influences of urea, pH and metal ions on the interaction between cepharanthine and lysozyme by steady state fluorescence spectroscopy. *J. Mol. Struct*. **2015**, *1084*, 229-235, DOI: 10.1016/ j.molstruc.2014.12.060.

[90] Das, S.; Ghosh, P.; Koley, S.; Roy, A. S., Binding of naringin and naringenin with hen egg white lysozyme: A spectroscopic investigation and molecular docking study, *Spectrochim. Acta A Mol. Biomol. Spectrosc*. **2018**, *192*, 211-221, DOI: 10.1016/j.saa.2017.11.015.

[91] Meti, M. D.; Nandibewoor, S. T.; Joshi, S. D.; More, U. A.; Chimatadar, S. A., Multi-spectroscopic investigation of the binding interaction of fosfomycin with bovine serumalbumin. *J. Pharm. Anal.* **2015***, 5* (4), 249-255, DOI: 10.1016/j.jpha.2015.01.0 04.